

## Accepted Manuscript

Rationally introduce AIE into chemosensor: A novel and efficient way to achieving ultrasensitive multi-guest sensing

Yan-Yan Chen, Qi Lin, You-Ming Zhang, Hong Yao, Tai-Bao Wei, Yan-Qing Fan, Xiao-Wen Guan, Guan-Fei Gong, Qi Zhou



PII: S1386-1425(19)30389-0

DOI: <https://doi.org/10.1016/j.saa.2019.04.014>

Reference: SAA 17022

To appear in: *Spectrochimica Acta Part A: Molecular and Biomolecular Spectroscopy*

Received date: 27 January 2019

Revised date: 4 April 2019

Accepted date: 9 April 2019

Please cite this article as: Y.-Y. Chen, Q. Lin, Y.-M. Zhang, et al., Rationally introduce AIE into chemosensor: A novel and efficient way to achieving ultrasensitive multi-guest sensing, *Spectrochimica Acta Part A: Molecular and Biomolecular Spectroscopy*, <https://doi.org/10.1016/j.saa.2019.04.014>

This is a PDF file of an unedited manuscript that has been accepted for publication. As a service to our customers we are providing this early version of the manuscript. The manuscript will undergo copyediting, typesetting, and review of the resulting proof before it is published in its final form. Please note that during the production process errors may be discovered which could affect the content, and all legal disclaimers that apply to the journal pertain.

**Rationally introduce AIE into chemosensor: a novel and efficient way to achieving ultrasensitive multi-guest sensing**

*Yan-Yan Chen<sup>a</sup>, Qi Lin<sup>a,\*</sup>, You-Ming Zhang<sup>a,b,\*</sup>, Hong Yao<sup>a</sup>, Tai-Bao Wei<sup>a</sup>, Yan-Qing Fan<sup>a</sup>,  
Xiao-Wen Guan<sup>a</sup>, Guan-Fei Gong<sup>a</sup>, Qi Zhou<sup>a</sup>*

*<sup>a</sup> Key Laboratory of Eco-Environment-Related Polymer Materials, Ministry of Education of China; Research Center of Gansu Military and Civilian Integration Advanced Structural Materials; College of Chemistry and Chemical Engineering, Northwest Normal University, Lanzhou, Gansu, 730070, China.*

*<sup>b</sup> College of Chemistry and Chemical Engineering, Lanzhou City University, Lanzhou, Gansu, 730070, China.*

Key words: ultrasensitive detection; AIE-based chemosensor; multi-analyte; aggregation induced emission enhancement (AIE); aroyl hydrazone

Corresponding authors: Pro. Dr. Qi Lin - linqi2004@126.com; Pro. Dr. You-Ming Zhang - zhangnwnu@126.com.

**Abstract:**

Recently, ultrasensitive detection and multi-guest sensing have received extensive attention due to their high sensitivity and efficiency. Herein, we report a novel approach to achieve ultrasensitive detection of multi-analyte. This approach is concluded as “rationally introduce Aggregation-Induced Emission (AIE) into chemosensor”. According to this approach, by rationally introducing self-assembly moiety, the obtained chemosensor **DNS** could serve as a novel AIEgen and show strong AIE in DMSO/H<sub>2</sub>O (water fraction 80%) binary solution. Interestingly, a simple fluorescent sensor array based on the **DNS** has been developed. This sensor array could selectively sense Fe<sup>3+</sup>, Al<sup>3+</sup>, H<sub>2</sub>PO<sub>4</sub><sup>-</sup> and L-Arg in water solution. More importantly, this sensor array shows ultrasensitive detection for Fe<sup>3+</sup>, Al<sup>3+</sup> and L-Arg. The LODs of the sensor array for Fe<sup>3+</sup>, Al<sup>3+</sup> and L-Arg are in the range of  $3.54 \times 10^{-9}$  M to  $9.42 \times 10^{-9}$  M. Moreover, H<sub>2</sub>PO<sub>4</sub><sup>-</sup> could realize the reversible detection of Fe<sup>3+</sup> in the DMSO/H<sub>2</sub>O (water fraction 80%) solution. Meanwhile, **DNS**-based test papers and thin films were prepared, which could serve as test kits for convenient detection Fe<sup>3+</sup>, Al<sup>3+</sup>, and L-Arg in water. In addition, they could also act as efficient erasable fluorescent display materials.

## 1 Introduction

In recent years, ultrasensitive response has gained extensive attentions due to their vital applications [1-6]. So far, many methods have developed to achieving ultrasensitive response for various guests. For instance, Jiang et al. [7] prepared two fluorescent probes for ultra-high sensitive detection hypochlorite acid (HOCl). Govindaraju et al. [8] proposed a novel optoelectronic approach based on nanoarchitectonics of small-molecule templated DNA system for ultrasensitive response of mercury. Therefore, it's still an intriguing issue to develop novel and efficient way for ultrasensitive sensing important analytes.

In addition, because ions and amino acids play significant roles in chemical, biological and environmental fields [9-12], ultrasensitive detection special ions and amino acids is needed. For example,  $\text{Fe}^{3+}$  is an essential transition metal ion in the human body, the deficiency or nimiety of  $\text{Fe}^{3+}$  in human body could result in pathological diseases [13, 14]. In addition, the excessive  $\text{Al}^{3+}$  in the body might restrain the uptake of other essential trace element, which would cause multifarious health problems, including Alzheimer's disease and Parkinson's disease [15-17]. Moreover, as the most alkaline amino acid, arginine plays vital role in biological functions and it is related to the pathogenesis of many cardiovascular disorders such as atheroma, hypertension and diabetes [18-22]. Therefore, it's very meaningful to develop methods for ultrasensitive and selective recognition of these important ions and amino acids in environmental or living cells.

In the past decades, since Tang et al. proposed the concepts of "Aggregation-Induced Emission" (AIE), the applications on AIE have gained increasing attentions [23, 24]. The AIE is a phenomenon that some compounds showed no/weak fluorescence emission in good solvent but highly emissive in the aggregated state [25]. Based on this pioneering research and other numerous fundamental studies, AIE has shown extensive applications in fluorescent sensors [26-28], organic light-emitting diodes (OLED) [29], light harvesting, bio-imaging and so on [30-32]. In addition, fluorogens with aggregation induced emission characteristics (AIEgens) have been served as a diverse and strong tool for sensing and imaging of versatile analytes including pH [33], ions [34], gas [35], biomolecules [36] and different processes, such as self-assembly [37-41]. Therefore, the rapid development of the AIE supplied good opportunity for design novel method to achieving ultrasensitive multi-guest detection. However, rationally introducing AIE into small molecule

chemosensors and using them for ultrasensitive detection of multi-analyte is rarely reported.

In view of these, and based on our research interests in ions and molecules recognition [42-49], herein, we report a novel approach to achieving ultrasensitive detection of multi-guest. This approach is concluded as “rationally introduce AIE into chemosensor”. Our strategies are as follows: firstly, in order to achieve the aggregation of the chemosensor, we rationally introduced multiple self-assemble driving forces, such as strong van der Waals force (through the long alkyl chain),  $\pi$ - $\pi$  stacking (through the aromatic groups) and multiple hydrogen bondings (through the acyl hydrazone group). Secondly, naphthalene was employed as an efficient fluorogen for the purpose of producing AIE. Moreover, the acylhydrazone group was introduced as multi-guest recognition site. Benefited from this rational design, as shown in Scheme 1-2, the obtained chemosensor **DNS** could act as a novel AIEgen and show strong AIE in DMSO/H<sub>2</sub>O (water fraction 80%) binary solution. Interestingly, the simple **DNS**-based fluorescent sensor array was constructed, which could selectively sense Fe<sup>3+</sup>, Al<sup>3+</sup>, H<sub>2</sub>PO<sub>4</sub><sup>-</sup> and L-Arg in water solution. More importantly, the chemosensor **DNS** shows ultrasensitive response properties for sensing Fe<sup>3+</sup>, Al<sup>3+</sup> and L-Arg in different aqueous systems. The LODs of the sensor for Fe<sup>3+</sup>, Al<sup>3+</sup> and L-Arg range from  $3.54 \times 10^{-9}$  M to  $9.42 \times 10^{-9}$  M. Moreover, H<sub>2</sub>PO<sub>4</sub><sup>-</sup> could realize the reversible detection of Fe<sup>3+</sup> in the DMSO/H<sub>2</sub>O (water fraction 80%) solution. Furthermore, **DNS**-based test papers and thin films were prepared, which could serve as test kits for convenient detection Fe<sup>3+</sup>, Al<sup>3+</sup>, and L-Arg in water. In addition, the **DNS** could also act as efficient erasable fluorescent display materials.

## 2 Experimental sections

### 2.1 Materials

All initial reagents and solvents were commercially available at analytical grade and were used without further purification. All metal ions were used from their perchlorate salts. All anions were used from their tetrabutylammonium salts, which were purchased from Alfa Aesar and used as received. All amino acids were purchased from Aladdin. Fresh double distilled water was used throughout the experiment.

### 2.2 Instruments

Melting points were measured on an X-4 digital melting-point apparatus (uncorrected). NMR

spectra were recorded on Varian Mercury-400 (400 MHz) and Varian Inova 600 instruments (600 MHz).  $^1\text{H}$  chemical shifts are reported in ppm downfield from tetramethylsilane (TMS, TM scale with the solvent resonances as internal standards). Mass spectra were performed on a Bruker Esquire 3000 plus mass spectrometer (Bruker-FranzenAnalytik GmbH Bremen, Germany) equipped with ESI interface and ion trap analyzer. The IR spectra were performed on a Digilab FTS-3000 Fourier transform-infrared spectrophotometer. Fluorescence spectra were recorded on a Shimadzu RF-5301PC spectrofluorophotometer. Ultraviolet-visible (UV-vis) spectra were recorded on a Shimadzu UV-2550 spectrometer.

## 2.3 Synthesis of AIEgen DNS

### 2.3.1 Synthesis of DN

Compound **D** was synthesized according to previous literature [50]. A solution of compound **D** (1.72 g, 5 mmol), methylparaben (0.91 g, 6 mmol),  $\text{K}_2\text{CO}_3$  (2.76 g, 20 mmol) and KI (0.33 g, 2 mmol) in 30 mL acetone was heated and stirred at 60 °C for 84 h. After the reaction was completed, the solid was filtered off and the solvent was collected, the filtrate was concentrated and recrystallized in acetone and pour water. Yield: 1.84 g, 89%; m. p. 117 ~ 120 °C;  $^1\text{H}$  NMR (600 MHz,  $\text{DCCl}_3$ , room temperature)  $\delta$  (ppm): 7.97 (d,  $J = 8.92$  Hz, 2H), 6.89 (d,  $J = 8.91$  Hz, 2H), 6.82 (m, 4H), 3.91 (s, 3H), 3.79 (s, 3H), 1.80 (m, 5H), 1.48 (m, 5H), 1.36 (m, 6H); ESI-MS  $m/z$ :  $[\text{DN} + \text{Na}]^+$  Calcd  $[\text{C}_{25}\text{H}_{34}\text{O}_5\text{Na}]^+$  437.23, found 437.27.

### 2.3.2 Synthesis of DNH

Hydrazine hydrate (0.3182 g, 6 mmol, 85%) was added into a solution of the **DN** (2.07 g, 5 mmol) in ethanol (150 mL). The mixture was heated in a round-bottomed flask at 85 °C for 12 h. The solvent was removed and the residue was recrystallized in ethanol. The product was collected by filtration, and dried under vacuum. Yield: 1.93 g, 93%; m. p. 147~151 °C;  $^1\text{H}$  NMR (400 MHz,  $\text{DCCl}_3$ , room temperature)  $\delta$  (ppm): 7.69 (d,  $J = 8.86$  Hz, 2H), 7.22 (s, 1H), 6.90 (d,  $J = 8.86$  Hz, 4H), 6.82 (s, 4H), 4.07 (s, 2H), 3.99 (t,  $J = 6.55$  Hz, 2H), 3.90 (t,  $J = 6.57$  Hz, 2H), 3.76 (s, 3H), 1.77 (m, 4H), 1.44 (m, 4H), 1.33 (m, 8H); ESI-MS  $m/z$ :  $[\text{DNH} + \text{Na}]^+$  Calcd  $[\text{C}_{24}\text{H}_{34}\text{N}_2\text{O}_4\text{Na}]^+$  437.24, found 437.26.

### 2.3.3 Synthesis of DNS

2-hydroxy-1-naphthaldehyde (0.34 g, 2 mmol) was added into a solution of the **DNH** (0.41 g, 1 mmol) in ethanol (50 mL), 2 mL acetic acid was added as catalyst. The mixture was heated in a

round-bottomed flask at 80 °C for 14 h. The solvent was removed and the residue was recrystallized in ethanol. The product was collected by filtration, and dried under vacuum. Yield: 0.41 g, 71%; m. p. 143~145 °C; <sup>1</sup>H NMR (400 MHz, DMSO-d<sub>6</sub>, room temperature) δ (ppm): 12.86 (s, 1H), 12.09 (s, 1H), 9.48 (s, 1H), 8.20 (d, J = 8.81 Hz, 1H), 7.96 (d, J = 9.02 Hz, 2H), 7.91 (d, J = 8.00 Hz, 2H), 7.62 (t, J = 8.00 Hz, 1H), 7.42 (t, J = 8.89 Hz, 1H), 7.24 (d, J = 8.89 Hz, 1H), 7.11 (d, J = 8.48 Hz, 1H), 6.83 (s, 4H), 4.07 (t, J = 6.42 Hz, 2H), 3.87 (t, J = 6.47 Hz, 2H), 3.68 (s, 3H), 1.70 (m, 4H), 1.41 (m, 4H), 1.31 (m, 8H); ESI-MS m/z: [DNS + H]<sup>+</sup> Calcd [C<sub>35</sub>H<sub>41</sub>N<sub>2</sub>O<sub>5</sub>]<sup>+</sup> 569.30, found 569.38.

#### Scheme 1.

### 3 Results and discussion

To observe the Aggregation-Induced Emission (AIE) properties of **DNS**, the fluorescence emission behaviors of the **DNS** were studied in the mixture of DMSO/H<sub>2</sub>O binary solution with different volume fractions of water. Because the DMSO is a good solvent for **DNS** while water is a poor solvent for **DNS**, as shown in Scheme 2b and Fig. 1, the low concentration **DNS** (DMSO, 1 × 10<sup>-4</sup> M) solution showed faint fluorescence emission, upon the addition of water into the DMSO solution of **DNS**, with the increase of the water volume fractions, the fluorescent emission intensity at 480 nm showed a gradual increase and reached the strongest state when the water volume fraction was at 80%. However, when the water contents reach to 90%, the fluorescence intensity of **DNS** was decreased, which could be attributed to the formation of precipitate when more water was added in the **DNS** (water fractions 80%) solution. Moreover, as shown in Scheme 2c, when **DNS** was dissolved in DMSO (1 × 10<sup>-4</sup> M), there is no Tyndall effect. However, with the gradual addition of water into the **DNS** solution, a distinct Tyndall effect could be observed. These phenomena indicated that **DNS** could aggregate in DMSO/H<sub>2</sub>O binary solution and the **DNS** showed AIE in DMSO/H<sub>2</sub>O (water fraction 80%) binary solution [23]. Meanwhile, fluorescence quantum yield of the **DNS** in DMSO/H<sub>2</sub>O (water fraction 80%) solution is calculated to be 0.36 (Fig. S7) according to the corresponding formula [51].

#### Scheme 2.

**Fig. 1.**

Moreover, the self-assembly mechanism of the **DNS** was studied by concentration  $^1\text{H}$  NMR spectra and SEM. Interestingly, as shown in Fig. 2, with the increasing of **DNS** concentration, the signals of H1 (at 12.87 ppm, Ar-OH), H2 (at 12.09 ppm, NH) and H3 (at 9.48 ppm, N=CH) showed distinct downfield shifts, which could be attributed to the formation of intramolecular hydrogen bond  $\text{C}=\text{N}\cdots\text{H}-\text{O}-\text{Ar}$  and intermolecular hydrogen bonds  $\text{C}=\text{O}\cdots\text{H}-\text{N}$  and  $\text{N}=\text{C}-\text{H}\cdots\text{O}-\text{Ar}$  (Scheme 2). These intermolecular hydrogen bonds induced the **DNS** self-assemble into one-dimensional supramolecular polymer. Meanwhile, the signals of H10 (at 7.11 ppm, Ar-H), H11 (at 6.83 ppm, Ar-H), H12 (at 4.07 ppm, Ar-O-CH<sub>2</sub>), H13 (at 3.87 ppm, Ar-O-CH<sub>2</sub>), H15 (at 1.71 ppm, -CH<sub>2</sub>), and H16 (at 1.42 ppm, -CH<sub>2</sub>) showed upfield shifts, which indicated that there are  $\pi$ - $\pi$  interactions [52] and van der Waals force existing in the aromatic rings and long alkyl chains on adjacent **DNS**. Therefore, the **DNS** could self-assemble into supramolecular system and form aggregation through intermolecular hydrogen bonds, van der Waals force and  $\pi$ - $\pi$  stacking effects. This proposed self-assembly mechanism also supported by SEM. As shown in Scheme 2d and 2e, the powder of **DNS** showed amorphous structure, however, the **DNS** solid obtained from the DMSO/H<sub>2</sub>O (80% water fraction) binary solution showed neat strips structure. This result also indicated that the **DNS** could aggregate in DMSO/H<sub>2</sub>O binary solution.

**Fig. 2.**

According to the above experiments, we speculate the self-assembly and AIE mechanism of the **DNS**. Before the molecule **DNS** aggregation, the long alkyl chain and acyl hydrazine group made the molecule conformationally flexible and underwent active intramolecular rotations, which could serve as a nonradiative transition channel for electrons from the excited states to the ground states [24]. While, after aggregation, the aggregated process limited the innate rotation of **DNS** by multiple noncovalent interactions (H-bond,  $\pi$ - $\pi$  stacking, and van der Waals force) and the radiationless pathway is blocked, meanwhile, the radiative channel is opened and emitted strong AIE fluorescence at 480 nm simultaneously [23, 24].

**Fig. 3.**

Then, the response abilities of **DNS** for different guests were studied in different water contents systems. Firstly, the cations response property of the **DNS** in DMSO/H<sub>2</sub>O (water fraction 80%)

solution was carefully investigated. For convenience, the DMSO/H<sub>2</sub>O (water fraction 80%) solution of **DNS** was named as **D80** in the after. Via adding and diffusing 10 equiv. various cations, including Mg<sup>2+</sup>, Ca<sup>2+</sup>, Cr<sup>3+</sup>, Fe<sup>3+</sup>, Co<sup>2+</sup>, Ni<sup>2+</sup>, Al<sup>3+</sup>, Cu<sup>2+</sup>, Zn<sup>2+</sup>, Ba<sup>2+</sup>, Ag<sup>+</sup>, Cd<sup>2+</sup>, Hg<sup>2+</sup>, and Pb<sup>2+</sup> (water solution, 0.1 M), into the **D80** solution, interestingly, only the addition of Fe<sup>3+</sup> induced the fluorescence of the **D80** “turned off”, and other cations did not show a similar response (Fig. 3 and 4a), which indicated that the **D80** could selectively fluorescence detect Fe<sup>3+</sup>. Then, the Fe<sup>3+</sup> specific selectivity of **D80** over other competitive cations was investigated by competitive experiment (Fig. S8). The results showed that the competitive cations did not lead to any significant influence in Fe<sup>3+</sup> sensing process. Furthermore, according to the fluorescent titration experiments (Fig. S10) and calculation based on the 3 $\sigma$ /m method [53], the limit of detection (LOD) of the **D80** for Fe<sup>3+</sup> is  $9.42 \times 10^{-9}$  M, which indicated that the sensor **D80** could ultrasensitively detect Fe<sup>3+</sup> (Fig. S9 and S11).

**Fig. 4.**

Due to the Fe<sup>3+</sup> quenching the AIE fluorescence of **D80**, the successive anions sensing properties of **DNS-Fe<sup>3+</sup>** complex (named as **D80Fe**) was carried out in DMSO/H<sub>2</sub>O (water fraction 80%) solution. Upon the addition of various anions (including F<sup>-</sup>, Cl<sup>-</sup>, Br<sup>-</sup>, I<sup>-</sup>, HSO<sub>4</sub><sup>-</sup>, H<sub>2</sub>PO<sub>4</sub><sup>-</sup>, N<sub>3</sub><sup>-</sup>, CN<sup>-</sup>, ClO<sub>4</sub><sup>-</sup>, SCN<sup>-</sup>, AcO<sup>-</sup>, S<sub>2</sub><sup>2-</sup>, 0.1 M, in water) into the **D80Fe** solution, as shown in Fig. 3, 4b and S12, only the addition of H<sub>2</sub>PO<sub>4</sub><sup>-</sup> could induce the fluorescence of **D80Fe** “turn-on”. This result indicated that the **D80Fe** could selectively detect H<sub>2</sub>PO<sub>4</sub><sup>-</sup>. And the LOD of the **D80Fe** for H<sub>2</sub>PO<sub>4</sub><sup>-</sup> is  $2.41 \times 10^{-7}$  M (Fig. S9, S13 and S14), which indicated a highly sensitive detection for H<sub>2</sub>PO<sub>4</sub><sup>-</sup>. Furthermore, the reversibility of the chemosensor function was tested by alternate adding Fe<sup>3+</sup> and H<sub>2</sub>PO<sub>4</sub><sup>-</sup> into the **D80** solution. As shown in Fig. S15, the fluorescent emission of **D80** solution showed alternating quenching and enhancing processes in a sequence, and the reversible process could be repeated at least three times with little fluorescent efficiency loss. Hence, the sensor **D80** could be considered as an “**OFF-ON-OFF**” fluorescent switch.

In addition, because the fluorescence emission of **DNS** solution under the 20% (including 20%) water volume fraction is very weak, so, a series of host-guest recognition property of **DNS** in the DMSO/H<sub>2</sub>O (water fraction 20%) solution was carried out and the system was named as **D20** in the after. At first, we investigated the recognition property of the **D20** toward various cations

through similar methods. After adding and diffusing 10 equiv. of various cations into the solution of **D20**, as shown in Fig. 5a, only the addition of  $\text{Al}^{3+}$  could enhance the fluorescence of **D20**. Meanwhile, other cations did not induce a similar response (Fig. 3). Therefore, the **D20** could selectively sense  $\text{Al}^{3+}$  through fluorescence enhancement way. As shown in Fig. S16, the LOD of the **D20** for  $\text{Al}^{3+}$  was obtained by fluorescent titration and calculated to be  $3.54 \times 10^{-9}$  M (Fig. S9 and S17), this result indicated that the detection of **D20** for  $\text{Al}^{3+}$  reached to ultrasensitive level.

**Fig. 5.**

Moreover, the successive response property of the complex **DNS- $\text{Al}^{3+}$**  toward various metal ions was studied in the DMSO/ $\text{H}_2\text{O}$  (water fraction 20%) solution of the **DNS- $\text{Al}^{3+}$**  (the system was named as **D20Al**) via similar method. As shown in Fig. 3, 5b and S18, only the addition of  $\text{Fe}^{3+}$  could make the fluorescence **D20Al** “turn off” and the other metal ions have no similar response, which indicated the **D20Al** could selectively detect  $\text{Fe}^{3+}$ . And the LOD of the **D20Al** for  $\text{Fe}^{3+}$  was calculated to be  $4.75 \times 10^{-8}$  M (Fig. S9, S19 and S20).

**Fig. 6**

Furthermore, it is well known that amino acids are the most basic substances which have close relationship with biological activities. So, we investigated the recognition property of **D20** toward various amino acids, including L-Phe, L-Gln, L-Ile, L-Thr, L-Glu, L-Ala, L-Ser, L-Met, L-Val, L-Tyr, L-Arg, L-Asp, L-Pro, L-His, L-Leu, L-Gly, L-Trp, L-Asn, and L-Cys (water solution, 0.1 M), by similar methods. As shown in Fig. 3 and 6, the **D20** could selectively dual-channel detect L-Arg by fluorescence increase and color change. Meanwhile, the competitive experiments also demonstrated that other amino acids couldn't induce any significant influence for the recognition process of L-Arg (Fig. S21 and S22). In addition, the fluorescence and UV-vis LODs of the **D20** for L-Arg were measured by fluorescence and UV-vis titrations (Fig. S23 and S25) and calculated to be  $8.97 \times 10^{-9}$  M and  $8.25 \times 10^{-9}$  M, respectively (Fig. S9, S24 and S26), which indicated ultrasensitive sensing for L-Arg.

According to the above results, as shown in Fig. 3, a novel sensor array based on **DNS** was successfully constructed. The sensor array could sense different guests: firstly, the **D80** could ultra-sensitively detect  $\text{Fe}^{3+}$ , meanwhile, the **D80Fe** could act as a new sensor to detect  $\text{H}_2\text{PO}_4^-$ .

Secondly, the **D20** could ultrasensitively sense  $\text{Al}^{3+}$  and L-Arg by the fluorescence enhanced. In addition, **D20** also showed colorimetric sensing property for L-Arg. Furthermore, the **D20Al** could be employed as a new sensor to sense  $\text{Fe}^{3+}$  with high selectivity and sensitivity. Based on these results, a novel four units sensor array was constructed, which could selectively and sensitively detect  $\text{Fe}^{3+}$ ,  $\text{H}_2\text{PO}_4^-$ ,  $\text{Al}^{3+}$  and L-Arg in aqueous solutions.

Then, the recognition mechanisms of the **DNS** for different guests were investigated by FT-IR,  $^1\text{H}$  NMR, ESI-MS and SEM experiments. At first, the recognition mechanism of **D80** for  $\text{Fe}^{3+}$  and  $\text{H}_2\text{PO}_4^-$  were investigated. In the IR spectra (Fig. S27), the stretching vibrational peaks appeared at 3435, 3221, 1647 and 1547  $\text{cm}^{-1}$  are assigned to the vibrational absorption peaks of NH, OH, C=O, and C=N groups of **DNS**, respectively. However, in the mixture of **D80** and  $\text{Fe}^{3+}$ , the OH vibration band disappeared, the C=O, and C=N vibration absorption peaks shifted to 1634  $\text{cm}^{-1}$  and 1537  $\text{cm}^{-1}$ , which indicated that upon the addition of  $\text{Fe}^{3+}$ , the **DNS** chelated with  $\text{Fe}^{3+}$  through the oxygen atom of C=O, the nitrogen atom of the C=N group and the oxygen of Ar-O. Meanwhile, the coordination process destroyed the self-assembly and aggregation of **DNS** and a significant emission quenching was observed after complexing with  $\text{Fe}^{3+}$  (Scheme 3). In the ESI-MS (Fig. S31), a peak at  $m/z$  1190.51 for  $[\text{2DNS} - 2\text{H} + \text{Fe}]^+$  was observed, which revealed a 2:1 stoichiometry for the complexation between **DNS** and  $\text{Fe}^{3+}$ . Furthermore, in the SEM image, after adding  $\text{Fe}^{3+}$ , the morphological feature of **D80** changed from neat strips to amorphous powder, this result also support the proposed  $\text{Fe}^{3+}$  coordination mechanism. Moreover, after adding  $\text{H}_2\text{PO}_4^-$  (1.0 M,  $\text{H}_2\text{O}$ ) into the **D80Fe**, in the FT-IR (Fig. S27), the OH vibration recovered, the C=O and C=N vibration absorption peaks shifted to 1650  $\text{cm}^{-1}$  and 1545  $\text{cm}^{-1}$ . Meanwhile, the corresponding SEM images changed from amorphous powder to layer (Fig. S30b and c). These results indicated that  $\text{H}_2\text{PO}_4^-$  competitively coordinated with  $\text{Fe}^{3+}$  in the **D80** and destroyed the complex of **DNS-Fe}^{3+}, meanwhile, the **DNS** self-assembled into an aggregation state and the AIE recovered again. (Scheme 3).**

In addition, the response mechanisms of **D20** for  $\text{Al}^{3+}$  and **D20Al** for  $\text{Fe}^{3+}$  were also investigated. Firstly, in the  $^1\text{H}$  NMR titration spectra (Fig. S28), after the addition of 1.0 equiv. of  $\text{Al}^{3+}$ , the single of naphthol OH peak at 12.87 ppm disappeared due to the deprotonation of sensor **DNS**. What's more, after adding more equivalents of  $\text{Al}^{3+}$ , new proton peaks appeared around H3-8 and H10, and all the new peaks showed downshifts. These new proton peaks could be

attributed to the  $\text{Al}^{3+}$  coordination inducing downshifts of the H3-8 and H10 and forming new peaks. Moreover, as shown in Fig. S32, in the ESI-MS, a peak at  $m/z$  297.13 for  $[\text{DNS} - \text{H} + \text{Al}]^{2+}$  was observed, which revealed a 1 : 1 stoichiometry for the complexation between **DNS** and  $\text{Al}^{3+}$ . To sum up, upon the addition of  $\text{Al}^{3+}$ , the **DNS** coordinate with  $\text{Al}^{3+}$  through the oxygen atom of  $\text{C}=\text{O}$ , the nitrogen atom of the  $\text{C}=\text{N}$  group and the oxygen of  $\text{Ar}-\text{O}$  (Scheme 3), which induced a significant emission enhancement. However, as shown in Fig. S30d, after adding  $\text{Fe}^{3+}$  to **D20Al**, the morphological feature of **D20Al** changed to amorphous powder. Based on the above study, as shown in Scheme 3, the proposed sensing of **D20Al** toward  $\text{Fe}^{3+}$  is a competitive coordination process between  $\text{Fe}^{3+}$  and  $\text{Al}^{3+}$ . Due to the stronger coordination property of  $\text{Fe}^{3+}$ , after adding  $\text{Fe}^{3+}$  to the solution of **D20Al**,  $\text{Fe}^{3+}$  could replace  $\text{Al}^{3+}$  from **D20Al** and form more stable complex **DNS-Fe**.

Finally, the L-Arg response mechanism was studied by  $^1\text{H}$  NMR experiment. In the  $^1\text{H}$  NMR spectra (Fig. S29), after the addition of L-Arg (0.1 M, water solution), the singlets of naphthol OH and imide NH peak at 12.87 ppm and 12.09 ppm disappeared, meanwhile, the other peaks show upshifts. This result indicated that the naphthol OH and imide NH moiety of **DNS** underwent a deprotonation process, which induced the fluorescent enhancement of the **DNS** through ICT mechanism. (Scheme 3).

### Scheme 3.

Furthermore, the **DNS**-based test papers were prepared by immersing the filter paper into the **DNS** ( $\text{DMSO}/\text{H}_2\text{O}$ ,  $1 \times 10^{-3}$  M) solution and then drying in air. Interestingly, the test papers could serve as an efficient test kits for convenient detection of  $\text{Fe}^{3+}$ ,  $\text{Al}^{3+}$  and L-Arg in water. As shown in Fig. 7a, these test papers exhibit weak fluorescence emission; upon dipping the test papers into the different concentration (from  $1 \times 10^{-1}$  M to  $1 \times 10^{-9}$  M) of  $\text{Fe}^{3+}$ ,  $\text{Al}^{3+}$  and L-Arg solution, respectively, the test papers showed distinct fluorescence changes. The lowest response concentration of these test papers for  $\text{Fe}^{3+}$ ,  $\text{Al}^{3+}$  and L-Arg are  $1 \times 10^{-9}$  M,  $1 \times 10^{-8}$  M and  $1 \times 10^{-8}$  M, respectively.

In addition, the **DNS**-based thin films were obtained by immersing the silica plate into the **DNS** ( $\text{DMSO}/\text{H}_2\text{O}$ ,  $1 \times 10^{-3}$  M) solution and then drying in air. As shown in Fig. 7b, the thin films showed weak fluorescence under the UV lamp (365 nm), when writing on the film with a capillary

tube inhaling  $\text{Fe}^{3+}$  water solution, a dark fluorescent writing image appeared and the dark fluorescent writing image could be erased by brushing  $\text{H}_2\text{PO}_4^-$  on the film again. Meanwhile, the same experiment was tested by  $\text{Al}^{3+}$  and L-Arg, when writing on the film with  $\text{Al}^{3+}$  (0.1 M, water solution), a brilliant blue fluorescent writing image appeared, and the fluorescence enhanced after writing with the L-Arg (0.1 M) water solution. Therefore, the **DNS**-based thin films could act as efficient erasable fluorescent display materials.

**Fig. 7.**

Furthermore, as shown in Table 1, after comparison with other reported  $\text{Fe}^{3+}$ ,  $\text{Al}^{3+}$  and L-Arg selective sensors [15, 54-63], the sensor **DNS** is synthesized in simple, low cost and high yield. More importantly, many reported chemosensors only could sense single guest, while the sensor **DNS** showed selective and ultrasensitive response for multi-guest in different water content systems.

**Table 1.**

## 4 Conclusion

In summary, based on the “rationally introduce AIE into chemosensor” strategy, a novel AIE-based chemosensor **DNS** was synthesized. Interestingly, the obtained chemosensor **DNS** could aggregate and show strong AIE in the DMSO/ $\text{H}_2\text{O}$  (water fraction 80%) binary solution. In addition, the **DNS** could act as a novel fluorometric and colorimetric chemosensor to selectively detect  $\text{Fe}^{3+}$ ,  $\text{Al}^{3+}$ ,  $\text{H}_2\text{PO}_4^-$  and L-Arg in different aqueous systems. Moreover, **DNS**-based sensor array was constructed, which could conveniently and selectively sense multi-guest in water solution. More importantly, the sensor could ultrasensitively detect  $\text{Fe}^{3+}$ ,  $\text{Al}^{3+}$  and L-Arg, the LODs of the sensor for  $\text{Fe}^{3+}$ ,  $\text{Al}^{3+}$  and L-Arg could reach to  $10^{-9}$  M. Furthermore, **DNS**-based test papers and thin films were prepared, the test papers could serve as test kits for convenient detection  $\text{Fe}^{3+}$ ,  $\text{Al}^{3+}$  and L-Arg in water, meanwhile, the thin films could act as erasable fluorescent display materials. Overall, the concept “rationally introduce AIE into chemosensor” is a novel and efficient approach for design fluorescent chemosensors and materials to achieving ultrasensitive detection and multi-guest response.

## Acknowledgments

This work was supported by the National Natural Science Foundation of China (NSFC) (No. 21574104; 21662031; 21661028) and the Program for Changjiang Scholars and Innovative Research Team in University of Ministry of Education of China (IRT 15R56).

## References:

- 1) M. Kandiah, P. L. Urban, *Chem. Soc. Rev.* 42 (2013) 5299.
- 2) H. Li, D. X. Chen, Y. L. Sun, Y. B. Zheng, L. L. Tan, P. S. Weiss and Y. W. Yang, *J. Am. Chem. Soc.* 135 (2013) 1570.
- 3) A. T. Aron, K. M. Ramos-Torres, J. A. Cotruvo Jr and C. J. Chang, *Acc. Chem. Res.* 48 (2015) 2434.
- 4) B. Tan, H. Zhao, W. Wu, X. Liu, Y. Zhang and X. Quan, *Nanoscale* 9 (2017) 18699.
- 5) S. Oh, J. Kim, V. T. Tran, D. K. Lee, S. R. Ahmed, J. C. Hong, J. Lee, E. Y. Park, J. Lee, *ACS Appl. Mater. Interfaces* 10 (2018) 12534.
- 6) Z. H. Xu, Y. Wang, Y. Wang, J. Y. Li, W. F. Luo, W. N. Wu, Y. C. Fan, *Spectrochim. Acta A.* 212 (2019) 146.
- 7) Y. Jiang, G. S. Zheng, Q. Y. Duan, L. Yang, J. Zhang, H. T. Zhang, J. He, H. Y. Sun and D. Ho, *Chem. Commun.* 54 (2018) 7967.
- 8) P. Q. Yang, J. Pang, F. H. Hu, J. M. Peng, D. F. Jiang, Z. Y. Chu, W. Q. Jin, *Sens. Actuators. B* 276 (2018) 31.
- 9) K. L. Diehl and E. V. Anslyn, *Chem. Soc. Rev.* 42 (2013) 8596.
- 10) J. R. Askim, M. Mahmoudi and K. S. Suslick, *Chem. Soc. Rev.* 42 (2013) 8649.
- 11) W. W. He, L. Luo, Q. Y. Liu, and Z. B. Chen, *Anal. Chem.* 90 (2018) 4770.
- 12) L. Y. Wang, L. L. Yang, D. R. Cao, *Sens. Actuators B* 209 (2015) 536.
- 13) Y. Z. Liu, L. Q. Shangguan, H. Wang, D. Y. Xia and B. B. Shi, *Polym. Chem.* 8 (2017) 3783.
- 14) L. Y. Wang, G. P. Fang, D. R. Cao, *Sens. Actuators B* 207 (2015) 849.
- 15) Z. R. Guo, Q. F. Niu, T. D. Li, *Spectrochim. Acta A* 200 (2018) 76.
- 16) E. T. Feng, C. B. Fan, N. S. Wang, G. Liu, S. Z. Pu, *Dyes Pigments* 151 (2018) 22.
- 17) D. Maity, T. Govindaraju, *Chem. Commun.* 46 (2010) 4499.

- 18) P. Nayak, *Environ. Res.* 89 (2002) 101.
- 19) N. Guelzim, F. Mariotti, P. G. P. Martin, F. Lasserre, T. Pineau, D. Hermier, *Amino Acids* 41 (2011) 969.
- 20) M. A. R. Vermeulen, M. C. G. van de Poll, G. C. Ligthart-Melis, C. H. C. Dejong, M. P. van den Tol, P. G. Boelens, P. A. M. van Leeuwen, *Crit. Care Med.* 35 (2007) S568.
- 21) J. K. Stechmiller, B. Childress, L. Cowan, *Nutr. Clin. Pract.* 20 (2005) 52.
- 22) S. Khezri, M. Bahram, N. Samadi, *Anal. Methods* 9 (2017) 6513.
- 23) J. Mei, N. L. C. Leung, R. T. K. Kwok, J. W. Y. Lam, B. Z. Tang, *Chem. Rev.* 115 (2015) 11718.
- 24) J. Luo, Z. Xie, J. W. Y. Lam, L. Cheng, B. Z. Tang, H. Chen, C. Qiu, H. S. Kwok, X. Zhan, Y. Liu, *Chem. Commun.* 18 (2001) 1740.
- 25) D. Ding, K. Li, B. Liu, B. Z. Tang, *Acc. Chem. Res.* 46 (2013) 2441.
- 26) J. T. Yang, J. Chai, B. S. Yang, B. Liu, *Spectrochim. Acta A.* 211 (2019) 272.
- 27) M. Pannipara, A. G. Al-Sehemi, A. Irfan, M. Assiri, A. Kalam, Y. S. Al-Ammaria, *Spectrochim. Acta A.* 201 (2018) 54.
- 28) A. G. Al-Sehemi, A. Irfan, M. Pannipara, M. A. Assiri, A. Kalam, *Zeitschrift für Physikalische Chemie*, 2019, DOI: 10.1515/zpch-2018-1215.
- 29) Y. Y. Yuan, W. B. Wu, S. D. Xu, and B. Liu, *Chem. Commun.* 53 (2017) 5287.
- 30) J. Mei, Y. Hong, J. W. Y. Lam, A. Qin, Y. Tang, B. Z. Tang, *Adv. Mater.* 26 (2014) 5429.
- 31) S. W. Guo, Y. S. Song, Y. L. He, X. Y. Hu, and L. Y. Wang, *Angew. Chem. Int. Ed.* 57 (2018) 3163.
- 32) S. D. Xu, Y. Y. Yuan, X. L. Cai, C. J. Zhang, F. Hu, J. Liang, G. X. Zhang, D. Q. Zhang, B. Liu, *Chem. Sci.* 6 (2015) 5824.
- 33) S. S. Liow, H. Zhou, S. Sugiarto, S. F. Guo, M. L. S. Chalasani, N. K. Verma, J. W. Xu, X. J. Loh, *Biomacromolecules* 18 (2017) 886.
- 34) S. Chen, Y. Hong, Y. Liu, J. Liu, C. W. Leung, M. Li, R. T. Kwok, E. Zhao, J. W. Lam, Y. Yu, *J. Am. Chem. Soc.* 135 (2013) 4926.
- 35) H. Mehdi, W. T. Gong, H. M. Guo, M. Watkinson, H. Ma, A. Wajahat, G. L. Ning, *Chem. Eur. J.* 23 (2017) 13067.
- 36) Y. Liu, Y. Tang, N. N. Barashkov, I. S. Irgibaeva, J. W. Lam, R. Hu, D. Birimzhanova, Y. Yu,

- B. Z. Tang, *J. Am. Chem. Soc.* 132 (2010) 13951.
- 37) Y. Yuan, S. Xu, X. Cheng, X. Cai, B. Liu, *Angew. Chem. Int. Ed.* 55 (2016) 6457.
- 38) X. Xue, Y. Zhao, L. Dai, X. Zhang, X. Hao, C. Zhang, S. Huo, J. Liu, C. Liu, A. Kumar, *Adv. Mater.* 26 (2014) 712.
- 39) T. Nishiuchi, K. Tanaka, Y. Kuwatani, J. Sung, T. Nishinaga, D. Kim, M. Iyoda, *Chem. Eur. J.* 19 (2013) 4110.
- 40) B. Wang, N. He, B. Li, S. Jiang, Y. Qu, S. Qu, J. Hua, *Aust. J. Chem.* 65 (2012) 387.
- 41) B. Z. Tang, X. Zhan, G. Yu, P. P. Sze Lee, Y. Liu, D. Zhu, *J. Mater. Chem.* 11 (2001) 2974.
- 42) D. D. Tao, Q. Wang, X. S. Yan, N. Chen, Z. Li, Y. B. Jiang, *Chem. Commun.* 53 (2017) 255.
- 43) H. T. Feng, Y. X. Yuan, J. B. Xiong, Y. S. Zheng and B. Z. Tang, *Chem. Soc. Rev.* 47 (2018) 7452.
- 44) Q. Lin, T. T. Lu, X. Zhu, T. B. Wei, H. Li, and Y. M. Zhang, *Chem. Sci.* 7 (2016) 5341.
- 45) Q. Lin, K. P. Zhong, J. H. Zhu, L. Ding, J. X. Su, H. Yao, T. B. Wei, H. Li, and Y. M. Zhang, *Macromolecules* 50 (2017) 7863.
- 46) J. F. Chen, Q. Lin, Y. M. Zhang, T. B. Wei, *Chem. Commun.* 53 (2017) 13296.
- 47) Q. Lin, Y. Q. Fan, G. F. Gong, P. P. Mao, J. Wang, X. W. Guan, J. Liu, Y. M. Zhang, H. Yao and T. B. Wei, *ACS Sustainable Chem. Eng.* 6 (2018) 8775.
- 48) Q. Lin, Y. Q. Fan, L. Liu, J. Liu, Y. M. Zhang, H. Yao and T. B. Wei, *Chem. Eur. J.* 24 (2018) 777.
- 49) Q. Lin, X. M. Jiang, X. Q. Ma, J. Liu, H. Yao, Y. M. Zhang, T. B. Wei, *Sens. Actuators. B* 272 (2018) 139.
- 50) Z. B. Zhang, G. C. Yu, C. Y. Han, J. Y. Liu, X. Ding, Y. H. Yu, F. H. Huang, *Org. Lett.* 13 (2011) 4818.
- 51) D. Magde, R. Wong, P. G. Seybold, *Photochem. Photobiol.* 75 (2002) 327.
- 52) Y. Feng, Z. T. Liu, J. Liu, Y. M. He, Q. Y. Zheng, Q. H. Fan, *J. Am. Chem. Soc.* 131 (2009) 7950.
- 53) Analytical Methods Committee, *Analyst* 112 (1987) 199.
- 54) L. L. Li, H. F. Xiang, X. G. Zhou, M. L. Li, and D. Wu, *J. Chem. Educ.* 89 (2012) 559.
- 55) C. X. Yang, H. B. Ren, and X. P. Yan, *Anal. Chem.* 85 (2013) 7441.
- 56) R. Lv, Z. H. Y. Chen, X. Fu, B. Y. Yang, H. Li, J. Su, W. Gu, X. Liu, *J. Solid State Chem.* 259 (2018) 67.

- 57) M. Kumar, A. Kumar, M. S. H. Faizi, S. Kumar, M. K. Singh, S. K. Sahu, S. Kishor, R. P. John, *Sens. Actuators. B* 260 (2018) 888.
- 58) T. Anand, A. S. K. Kumar, S. K. Sahoo, *Spectrochim. Acta A.* 204 (2018) 105.
- 59) E. Feng, C. Fan, N. S. Wang, G. Liu, S. Z. Pu, *Dyes Pigments* 151 (2018) 22.
- 60) G. Patel and S. Menon, *Chem. Commun.* 0 (2009) 3563.
- 61) R. S. Bhosale, G. V. Shitre, R. Kumar, D. O. Biradar, S. V. Bhosale, R. Narayan, S. V. Bhosale, *Sens. Actuators. B* 241 (2017) 1270.
- 62) X. Q. Zeng, L. Zhang, J. D. Yang, Y. Guo, Y. M. Huang, H. Y. Yuan, and Y. S. Xie, *New J. Chem.* 41 (2017) 15216.
- 63) S. Khezri, M. Bahram, N. Samadi, *Anal. Methods.* 9 (2017) 6513.

## List of Schemes, Figures and Table:

**Scheme 1.** The synthesis of **DNS**.

**Scheme 2.** (a) The proposed AIE-induced self-assemble mechanism of the chemosensor **DNS**; (b) Fluorescence photographs of the **DNS** ( $1 \times 10^{-4}$  M) in DMSO and DMSO/H<sub>2</sub>O (water fraction 80%) solution. (c) Photos showing the Tyndall effect of **DNS** in DMSO and DMSO/ H<sub>2</sub>O (water fraction 80%) binary solution. (d) and (e) The SEM images of the powder **DNS** and **DNS** in the DMSO/H<sub>2</sub>O (water fraction 80%) solution.

**Fig. 1.** The fluorescence intensity of the **DNS** ( $1 \times 10^{-4}$  M,  $\lambda_{ex} = 365$  nm,  $\lambda_{em} = 480$  nm, Slit = 1.5/20 nm) in DMSO/H<sub>2</sub>O binary solution with different volumetric fractions of water (vol %).

**Fig. 2.** Partial <sup>1</sup>H NMR spectra (400 MHz, 298 K) of **DNS** in DMSO-*d*<sub>6</sub> with various concentration: (a) 10.0 (b) 40.0 (c) 80.0 and (d) 120.0 mg/mL.

**Fig. 3.** Multi-analyte response properties of **DNS**-based sensor array in different water aqueous for different ions and amino acids.

**Fig. 4.** (a) Fluorescence spectra of **D80** ( $1 \times 10^{-5}$  M) in the presence of an excess (10 equivalents) of various cations in mixed aqueous medium. (b) Fluorescence spectra of **D80Fe** ( $1 \times 10^{-5}$  M) in the presence of an excess (10 equivalents) of various cations in mixed aqueous medium ( $\lambda_{ex} = 365$  nm, Slit = 1.5/20 nm).

**Fig. 5.** (a) Fluorescence spectra of **D20** ( $1 \times 10^{-4}$  M) in the presence of an excess (10 equivalents) of various metal ions in mixed aqueous medium. (b) Fluorescence spectra of **D20Al** ( $1 \times 10^{-4}$  M) in the presence of an excess (10 equivalents) of various metal ions in mixed aqueous medium ( $\lambda_{ex} = 365$  nm, Slit = 3/1.5 nm).

**Fig. 6.** (a) Fluorescence spectra of **D20** ( $1 \times 10^{-4}$  M) in the presence of an excess (10 equivalents) of various amino acids in mixed aqueous medium ( $\lambda_{ex} = 365$  nm, Slit = 5/5 nm). (b) UV-vis absorption spectra of **D20** ( $1 \times 10^{-4}$  M) in the presence of an excess (10 equivalents) of various

amino acids in mixed aqueous medium.

**Scheme 3.** The proposed aggregation process of the chemosensor **DNS** and the recognition mechanisms to  $\text{Fe}^{3+}$ ,  $\text{Al}^{3+}$ , L-Arg and  $\text{H}_2\text{PO}_4^-$ .

**Fig. 7.** (a) Fluorescence changes of **DNS**-based test papers after addition different concentration (from  $1 \times 10^{-1}$  M to  $1 \times 10^{-9}$  M) of  $\text{Fe}^{3+}$ ,  $\text{Al}^{3+}$  and L-Arg. (b) Writing and erasing of a natural light invisible image on **DNS** thin films. The photographs were taken at room temperature under 365 nm ultraviolet light (UV).

**Table 1.** Comparison of the LODs of different chemosensors for analytes.

**Table 1.** Comparison of the LODs of different chemosensors for analytes.

Analytes	Refs	Solvents	LOD (nM)
Fe <sup>3+</sup>	54	Water	$1.40 \times 10^6$
	55	Aqueous Solution	$9.00 \times 10^2$
	56	Aqueous Solution	$3.00 \times 10^2$
	15	THF/H <sub>2</sub> O (water fraction 30%)	$1.72 \times 10^2$
	<b>This work</b>	<b>DMSO/H<sub>2</sub>O (water fraction 80%)</b>	<b>9.42</b>
	<b>This work</b>	<b>DMSO/H<sub>2</sub>O (water fraction 20%)</b>	<b>47.5</b>
Al <sup>3+</sup>	54	Water	$1.50 \times 10^4$
	57	CH <sub>3</sub> OH/H <sub>2</sub> O (water fraction 10%)	$4.32 \times 10^3$
	58	DMSO/H <sub>2</sub> O (water fraction 50%)	$2.90 \times 10^3$
	59	CH <sub>3</sub> CN	$5.50 \times 10^2$
	<b>This work</b>	<b>DMSO/H<sub>2</sub>O (water fraction 20%)</b>	<b>3.54</b>
L-Arg	60	Aqueous Solution	$4.00 \times 10^3$
	61	Aqueous Solution	$1.94 \times 10^3$
	62	Aqueous Solution	28.50
	63	Aqueous Solution	13.80
	<b>This work</b>	<b>DMSO/H<sub>2</sub>O (water fraction 20%)</b>	<b>8.97</b>
	<b>This work</b>	<b>DMSO/H<sub>2</sub>O (water fraction 20%)</b>	<b>8.25</b>

# Rationally introduce AIE into chemosensor: a novel and efficient way to achieving ultrasensitive multi-guest sensing

*Yan-Yan Chen<sup>a</sup>, Qi Lin<sup>a,\*</sup>, You-Ming Zhang<sup>a,b,\*</sup>, Hong Yao<sup>a</sup>, Tai-Bao Wei<sup>a</sup>,  
Yan-Qing Fan<sup>a</sup>, Xiao-Wen Guan<sup>a</sup>, Guan-Fei Gong<sup>a</sup>, Qi Zhou<sup>a</sup>*

## Highlights

1. A novel approach to realizing ultrasensitive detection multi-analyte.
2. Rationally induce AIE into the small molecular chemosensor.
3. A simple sensor array for  $\text{Fe}^{3+}$ ,  $\text{Al}^{3+}$ ,  $\text{H}_2\text{PO}_4^-$  and L-Arg was created.
4. Ultrasensitive detection for  $\text{Fe}^{3+}$ ,  $\text{Al}^{3+}$  and L-Arg in aqueous solutions.
5. LODs of the sensor array for  $\text{Fe}^{3+}$ ,  $\text{Al}^{3+}$  and L-Arg reached  $10^{-9}$  M.
6.  $\text{Fe}^{3+}$ ,  $\text{Al}^{3+}$ , L-Arg test papers and fluorescent display materials were prepared.

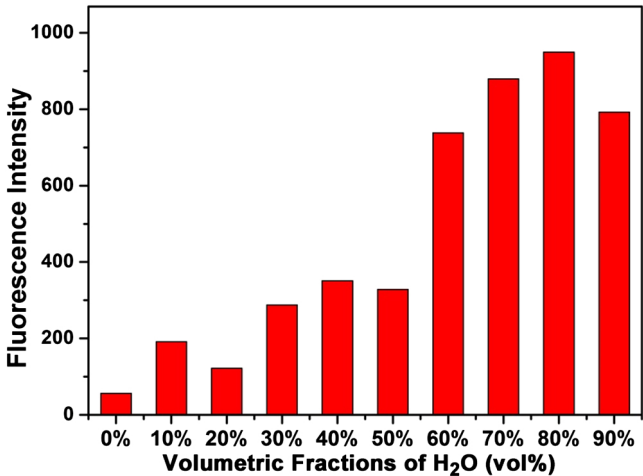


Figure 1

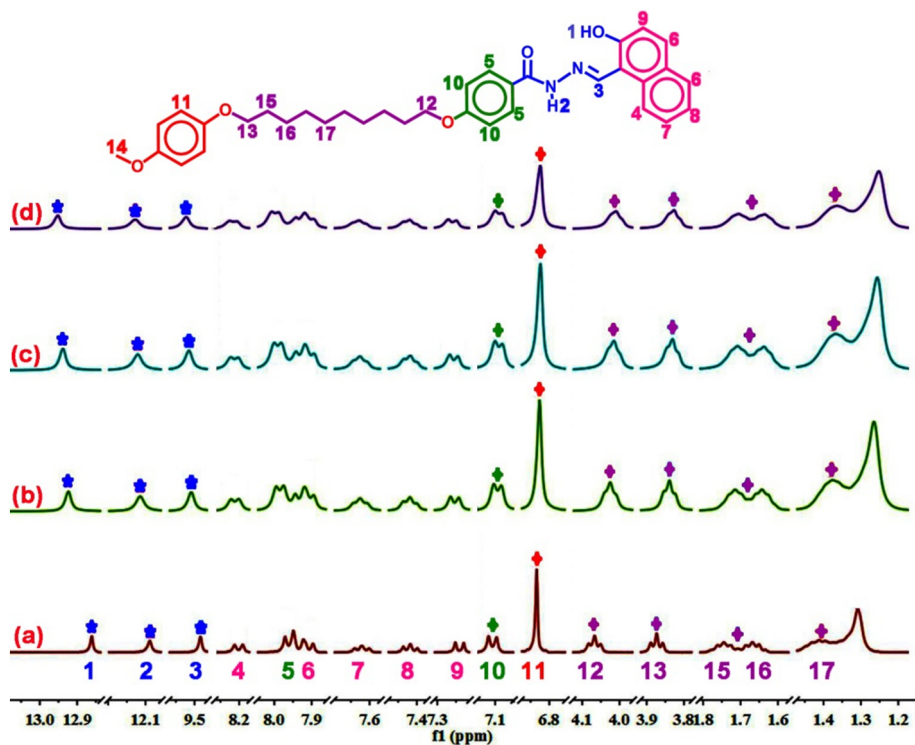


Figure 2

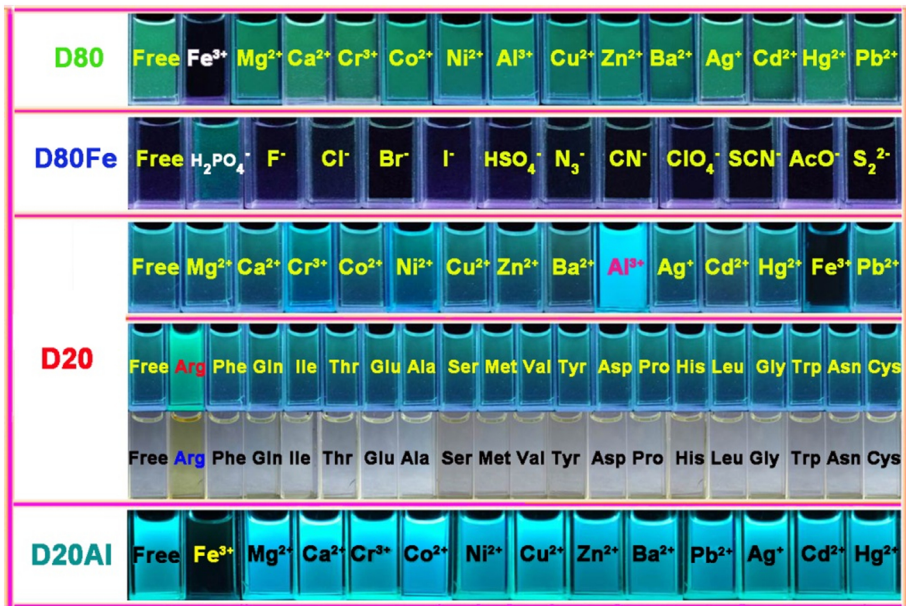


Figure 3

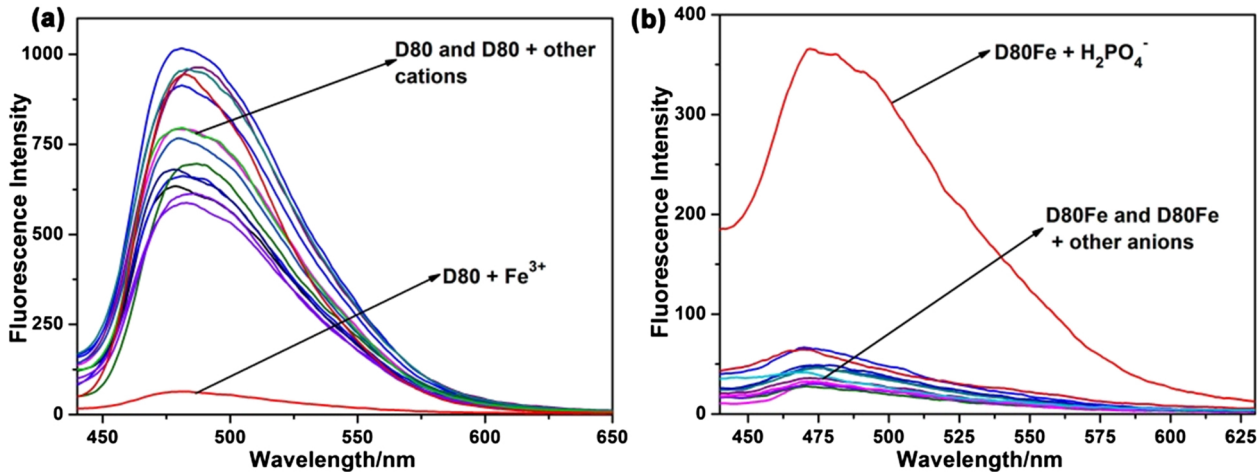


Figure 4

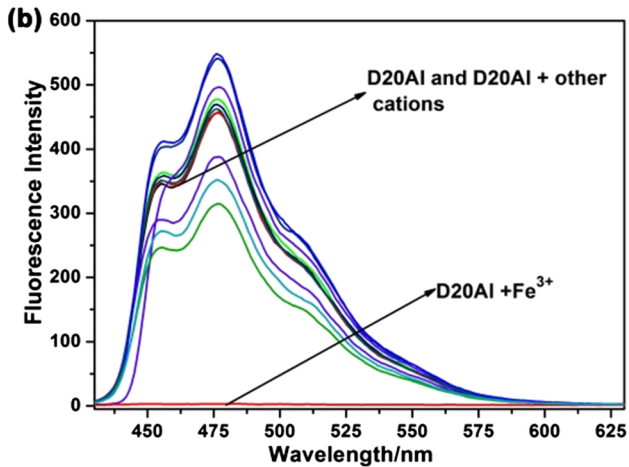
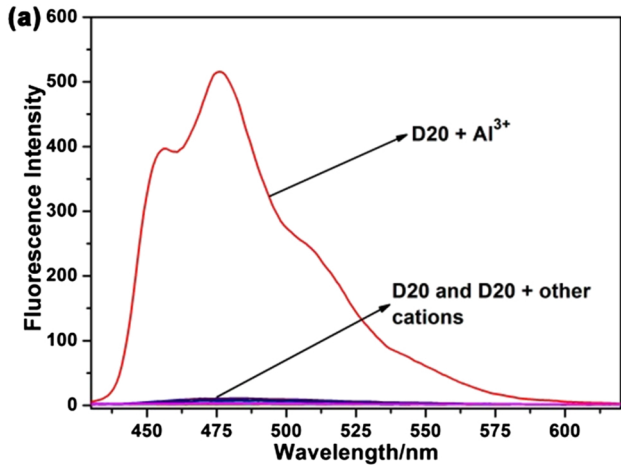


Figure 5

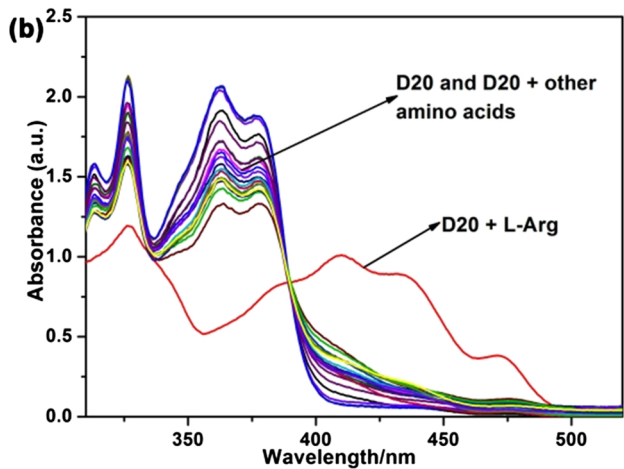
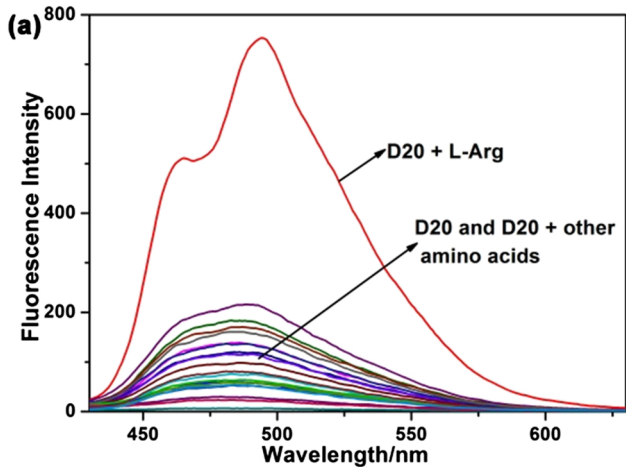


Figure 6

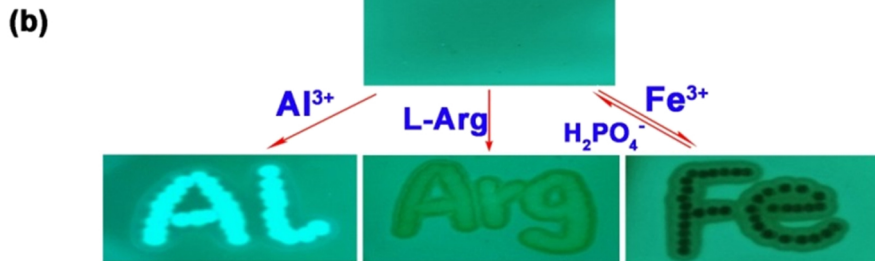
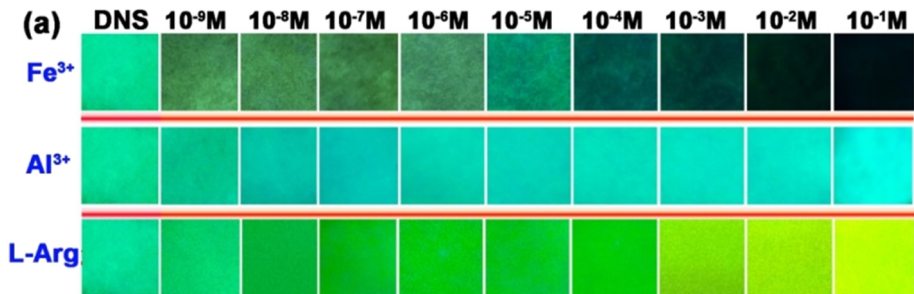


Figure 7